Effect of different HDTMA loading on silver modified kaolinite on its antibacterial activity

Cite as: AIP Conference Proceedings **2231**, 020003 (2020); https://doi.org/10.1063/5.0002423
Published Online: 22 April 2020

Muhammad Hariz Asraf, and Nik Ahmad Nizam Nik Malek

Effect of Different HDTMA Loading on Silver Modified Kaolinite on Its Antibacterial Activity

Muhammad Hariz Asraf[1,a)] and Nik Ahmad Nizam Nik Malek[1,2,b)]

[1]*Department of Biosciences, Faculty of Science, Universiti Teknologi Malaysia (UTM), 81310 UTM Johor, Malaysia*
[2]*Centre for Sustainable Nanomaterials (CSNano), Ibnu Sina Institute for Scientific and Industrial Research (ISI-ISIR), Universiti Teknologi Malaysia (UTM), 81310 UTM Johor, Malaysia*

[a)]mharizasraf@gmail.com
[b)]Corresponding author: niknizam@utm.my

Abstract. A synergistic combination of organic and inorganic materials as a hybrid antibacterial agent aiming to combine two or more antibacterial compounds in a carrier system has been developed. This research aimed to study the physicochemical properties of silver loaded kaolinite attached with different amounts of cationic surfactant hexadecyltrimethylammonium (HDTMA) and its effect on Gram-positive and Gram-negative bacteria. Kaolinite was initially modified with silver ion and later, with different HDTMA concentrations (50, 75, and 100% of Cation Exchange Capacity (CEC) of the kaolinite). The materials were characterized using X-ray diffraction, Fourier transforms infrared spectroscopy and field emission scanning electron microscope equipped with energy dispersive X-ray analyzer. Antibacterial activity was evaluated using disc diffusion technique against *Escherichia coli* and *Staphylococcus aureus*. Characterization results showed that kaolinite was successfully modified with silver ion and HDTMA. For the antibacterial assay, *S. aureus* was more susceptible than *E. coli* due to differences in their peptidoglycan structure, whereas, surfactant-modified silver kaolinite was more effective in inhibiting bacterial growth than silver kaolinite. However, the different concentrations of HDTMA did not alter the existing inhibitory effects against these bacteria. Thus, the low concentration of HDTMA loaded on silver-kaolinite is suitable to be used as an antibacterial agent.

INTRODUCTION

Bacteria such as *Escherichia coli* and other related species of Gram-negative bacteria have developed resistance towards a wide variety of antimicrobial agents either by intrinsic or acquired resistance [1]. This resistance is also due to the regular and continuous use of these agents against them. The adaptation has taken several long years to show its effect. Hence, the use of a single antibacterial agent has become less active to prevent microbial growth. Silver is the most popular antibacterial agent that has been used in ages for antibacterial testing and thus, making it prominent in many studies [2–4]. It will undoubtedly show its antibacterial effect on bacteria. However, does this property will be able to maintain its efficiency for an extended period.

In the meantime, clay, such as kaolinite, has been widely studied for its potential as a carrier agent [5]. A carrier denotes a host that can be modified or loaded with one or more compatible compounds. Generally, kaolinite consists of intercalating layers that allow it to be modified with certain compounds that fit into these layers. Besides that, kaolinite itself has elusive broken edges that give the negatively charged property to the surface of kaolinite and host to the common exchangeable cations such as Ca^{2+}, Mg^{2+}, $H^{+,}$ and more [6]. These charges enable ionic interaction to occur at the kaolinite surface while attracting positively charged particles or compounds. Henceforth, these properties that fit kaolinite as a carrier system prove its potential to carry more than one compound for various purposes, including antibacterial agents [7], phytonutrients for plant growth such as nitrogen [8], and also as an animal feed to enhance production [9].

International Conference on Life Sciences and Technology (ICoLiST)
AIP Conf. Proc. 2231, 020003-1–020003-6; https://doi.org/10.1063/5.0002423
Published by AIP Publishing. 978-0-7354-1990-2/$30.00

Hence, the multi-carrying property of kaolinite was tested by modifying more than one antibacterial agent for this project. The combination of two antibacterial agents, namely, silver (Ag) from silver nitrate and hexadecyltrimethylammonium (HDTMA) were tested on its proficiency in preventing microbial growth, especially on *E. coli* and *S. aureus*. Since Ag is a known antibacterial agent, the purpose was to further enhance the antibacterial effect by introducing several concentrations of HDTMA (50%, 75%, and 100%) from the original cationic exchange capacity (CEC) of the kaolinite.

EXPERIMENTAL DETAILS

The raw material used in this experiment was cosmetic grade kaolinite (KM88C) (Kaol) supplied by Kaolin (Malaysia) Sdn Bhd, which was initially treated before being distributed locally. The CEC of the Kaol that was calculated using the ammonium acetate method is 7.18 meq/100g. This value was used to calculate the amount of silver nitrate and HDTMA needed to be loaded into the raw kaolinite (Table 1).

TABLE 1. Amount of Ag and HDTMA for the preparation of HDTMA-Ag modified kaolinite.

Samples	Kaolinite (g)	$AgNO_3$ in dH_2O (g/500 mL)	HDTMA in dH_2O (g/500 mL)
Kaol	10.0	-	-
Ag-Kaol	10.0	0.0610	-
	Ag-Kaol (g)		
H-Ag-Kaol 50	5.0		0.0654
H-Ag-Kaol 75	5.0		0.0981
H-Ag-Kaol 100	5.0		0.1308

Characterizations of the samples were conducted using several instruments, including Field Emission Scanning Electron Microscope (FESEM) with Energy dispersive X-ray (EDX) analysis, Fourier Transform Infrared Spectroscopy (FTIR), and X-ray Powder Diffraction (XRD). The Bruker (D8 advance) XRD machine was operated using a step scanning program with a scanning speed of 0.05° per second, in the range of $2\theta = 5°$ to 50°. The XRD pattern was recorded with Cu-Kα radiation at $\lambda = 1.5406$ Å, at 40 kV, 20mA. The samples were also characterized using the Thermo Scientific Nicolet IS10 FTIR spectrometer with OMNIC™ software. It was done by using KBr pressed disc method. All the samples were scanned in the range of 4000 - 400 cm^{-1} for their FTIR spectra with a wavenumber resolution of 4 cm^{-1}. Lastly, The FESEM images were captured under the condition of LEI with 5.0 kV and WD 8.1 mm.

As for the assay, the disc diffusion technique (DDT) was utilized to assess the antibacterial property of the prepared samples. All required media including nutrient agar (NA) and Mueller-Hinton agar (MHA) were prepared prior to the culturing bacteria. *E. coli* ATCC 11229 and *Staphylococcus aureus* ATCC 6538 were used as model bacteria in this antibacterial assay. The prepared samples were initially pressed into disc-shaped pellets for the assay. Initially, five to ten single colonies of the bacteria were inoculated into a 0.9% saline solution. Within 15 minutes, the bacteria solution was compared to the prepared 0.5 McFarland standard and was adjusted according to its turbidity. A sterile cotton bud was used to dip into the bacterial solution and swab thoroughly onto the MHA to ensure evenly-distributed bacterial growth. The pellets were placed on the surface of MHA with the bacterial culture on it. The plate was incubated at 37°C overnight with an upside-down position. Later, the inhibition zone formed was measured using a conventional ruler (in cm) for all samples.

RESULTS AND DISCUSSION

The FTIR spectra of unmodified and modified kaolinite (Fig. 1) showed typical bands for kaolinite structure except for the newly appeared bands around 2800 cm^{-1} and 2900 cm^{-1}. After the modification of kaolinite with different concentrations of HDTMA, the bands at 2849 cm^{-1} and 2921 cm^{-1} started to appear contributed by the C-H bonds in the alkyl group of the HDTMA [12]. The band formations ranging from 1200 cm^{-1} to 400 cm^{-1} usually denote the fingerprint region of the kaolinite itself, confirming the presence of Si-O-Si (siloxane), Si-O-Al, hydroxyl groups, and aluminum-oxygen bonds [10]. The lattice water molecule band is also shown around the region of 1650 cm^{-1} [11]. After the addition of silver ion into the kaolinite, there is no chance of the spectra since the silver ions exist as ionic form and do not have any bonds. The presence of silver ion cannot be detected using FTIR. Therefore, the silver ion

is validated qualitatively by the presence of an inhibition zone for the Ag-Kaol sample and also using EDX. The HDTMA molecules were successfully attached to the kaolinite and Ag-kaolinite frameworks.

Figure 2 is the X-ray diffractogram of all the prepared samples. Each sample was characterized by XRD to compare the difference between unmodified and modified kaolinite in terms of its crystallinity. Based on the analysis, there are several noticeable peaks along 2θ degree that denotes the property of the kaolinite at 12.4°, 24.9°, 38.45°, and 45.4°. The basal spacing at 7.17 Å also denotes the typical kaolinite XRD pattern [13] with a quartz impurity at d = 3.35 Å. There is no significant change occurs on the XRD pattern after the modification of Ag and both Ag-HDTMA. This can be correlated with the FTIR spectra in Fig. 1 at the fingerprint region of the kaolinite, which clarifies that Ag and HDTMA did not alter the structural framework of kaolinite.

Based on the FESEM images (Fig. 3) of the raw kaolinite and modified kaolinite, all of the microscopic images show the basic and fundamental structure of kaolinite, which is the intercalating layer as mentioned previously. The surface of the samples shows a rough and complex structure with flaky interlayers, jagged small-size broken edges to support the adsorption of HDTMA [14]. By looking at the images, it is found that no distinct occurrence of the structural changes of the kaolinite at all magnifications. This means that the kaolinite still maintains its original structure even after modification. The elemental distribution obtained using EDX is tabulated in Table 2. As expected, all samples contain essential elements that made up kaolinite, which includes O, Si, and Al. On the other hand, the samples that were modified with Ag show the presence of the Ag element. On the contrary, this is an important benchmark, which indicates that Ag ions were successfully loaded into the kaolinite for all related samples.

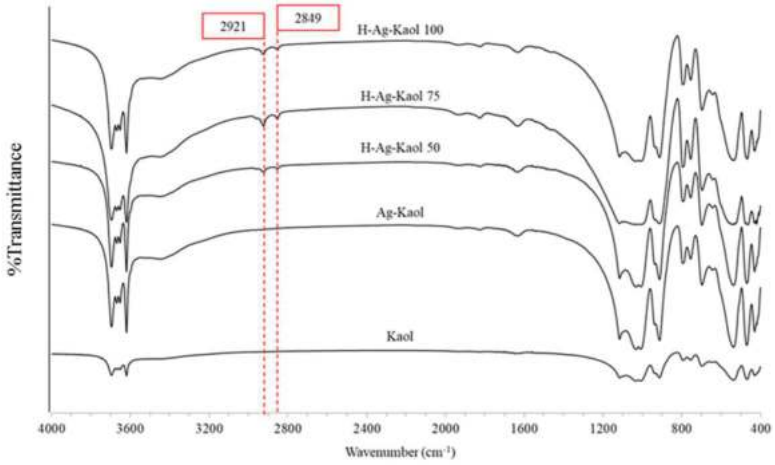

FIGURE 1. FTIR spectra of (from bottom) unmodified kaolinite, silver-modified kaolinite, HDTMA-silver modified kaolinite (50%), HDTMA-silver modified kaolinite (75%), and HDTMA-silver modified kaolinite (100%).

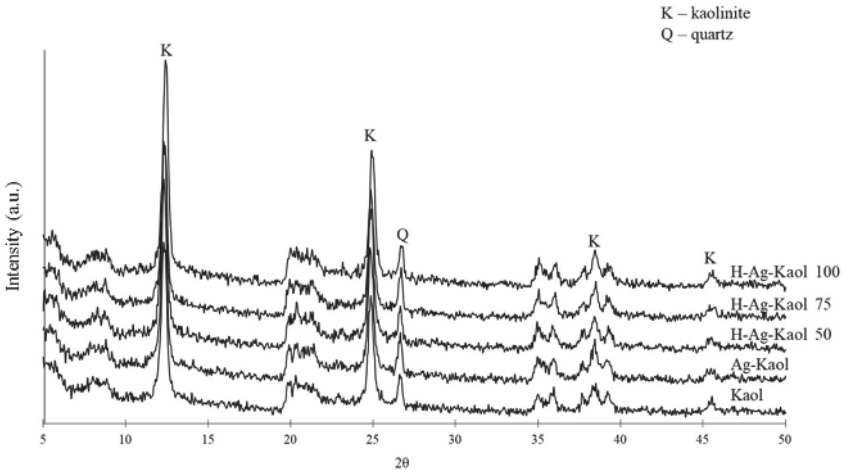

FIGURE 2 X-ray diffractogram of the prepared samples. From the bottom, unmodified kaolinite, silver-modified kaolinite, HDTMA-silver modified kaolinite (50%), HDTMA-silver modified kaolinite (75%), and HDTMA-silver modified kaolinite (100%).

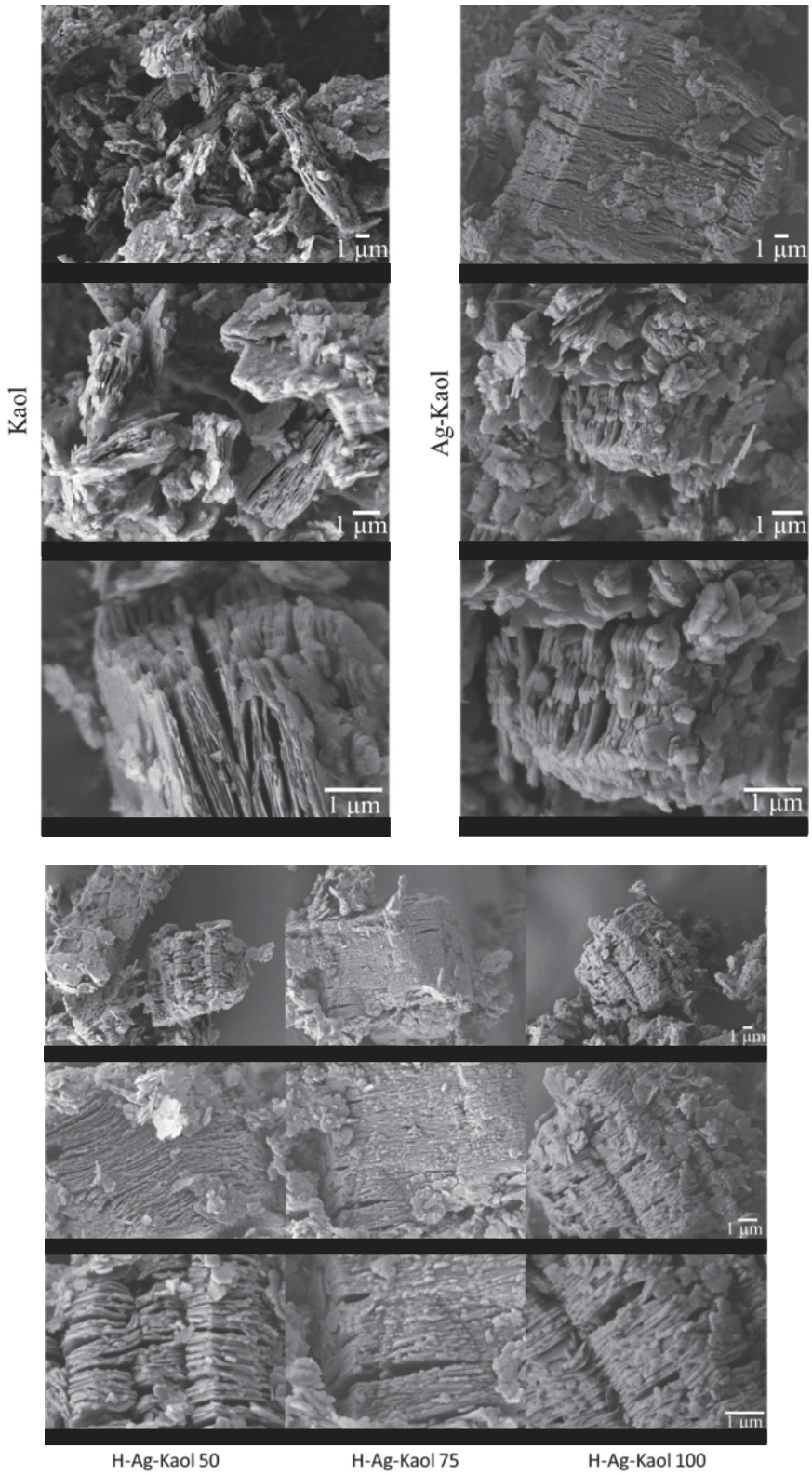

FIGURE 3. Morphology of the prepared samples. Different magnifications of 5K ×, 10K ×, and 20K × were visualized.

TABLE 2. Elemental distribution of unmodified Kaol and modified Kaol. Three spots were captured on the samples to derive standard deviations for three replicates reading.

Sample	Atomic mass (%)			
	Silica	Oxygen	Aluminium	Silver
Kaol	67.92 ± 2.62	5.76 ± 2.40	28.25 ± 1.49	-
Ag-Kaol	69.31 ± 6.02	13.84 ± 0.17	24.97 ± 1.08	1.75 ± 0.90
H-Ag-Kaol 50	38.18 ± 5.62	0.89 ± 1.55	15.33 ± 2.11	0.33 ± 0.29
H-Ag-Kaol 75	36.10 ± 3.24	6.70 ± 11.60	13.94 ± 0.97	7.52 ± 9.99
H-Ag-Kaol 100	38.23 ± 7.31	2.25 ± 3.90	17.23 ± 3.85	1.30 ± 1.84

The inhibition zones formation of the bacteria after interacting with the samples are shown in Fig. 4, while Table 3 gives the diameter of the inhibition zones (in cm). Based on Fig. 4 and Table 3, there is no formation of an inhibition zone for bacteria treated with raw kaolinite. It does not contain any antibacterial property and, thus, can only be used as a control sample for this experiment. However, the antibacterial effect started to show its role after the kaolinite was modified with Ag. The zone of inhibition also portrays further expansion after the addition of HDTMA molecules. According to the finding, *S. aureus* is more susceptible compared to *E. coli*. However, different concentration of HDTMA does not contribute to the change of the inhibition zone.

The type of bacteria themselves is contributing to this susceptibility. For instance, *E. coli* is a gram-negative bacterium while *S. aureus* is a gram-positive bacterium. These features can determine the resistance of both bacteria. When both bacteria were tested with silver-modified kaolinite, they show an almost equal inhibition zone diameter, which is around 1.6 ± 0.1 and 1.7 ± 0.0, respectively. However, after the bacteria were treated with HDTMA-silver modified kaolinite, a significant increase in inhibition zone diameter can be observed for *S. aureus* but not *E. coli*. This is an intriguing finding which shows that this *E. coli* ATCC 11229 has slight resistance towards HDTMA. Contradictorily, *S. aureus* is significantly more susceptible when came into contact with HDTMA.

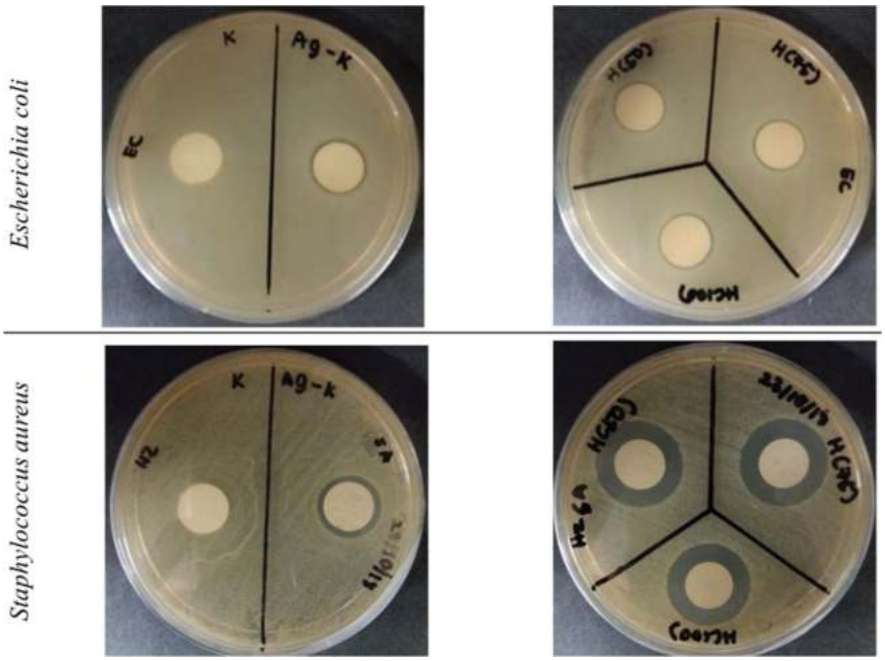

FIGURE 4 The inhibition zones (in cm) of *E. coli* and *S. aureus* after being treated with the respective samples.

This can be explained through the mechanism of Ag to alter the membrane of bacteria. Silver, as in Ag ions, carries a positive charge, which then can interact via ionic interaction with the negatively-charged bacterial membrane. Thus, this alteration disrupts the ability to replicate the DNA molecules and inactivate related proteins through the interaction between Ag ion and the protein thiol group [15]. Generally, Gram harmful bacteria should be more susceptible due to their weak peptidoglycan layers to protect their essential cell content. After HDTMA molecules were introduced into the sample, *S. aureus,* which is a gram-positive bacterium, depicts more susceptibility towards the compound. It can

be deduced that the synergistic effects of Ag and HDTMA work miraculously to prevent the growth of *S. aureus*. This finding is similar to that HDTMA-copper kaolinite that was tested on both *E. coli* and *S. aureus* in which the gram-positive bacteria exhibited total resistance towards the material and otherwise for the gram-positive bacteria [16]. In this case, the HDTMA in the samples might directly attack the peptidoglycan layer/cell wall of the *S. aureus,* making it loses its function and allows Ag to penetrate deeper into the cytoplasm, altering its cell system and eventually leads to cell death.

TABLE 3. The inhibition zones (in cm) of each sample tested with raw kaolinite, silver-modified kaolinite, and HDTMA-silver modified kaolinite of different HDTMA concentrations.

Bacteria	Samples				
	Kaol	Ag-Kaol	HDTMA-Ag-Kaol 50	HDTMA-Ag-Kaol 75	HDTMA-Ag-Kaol 100
E. coli	NA	1.6 ± 0.1	1.4 ± 0.0	1.4 ± 0.1	1.4 ± 0.0
S. aureus	NA	1.7 ± 0.0	2.2 ± 0.1	2.3 ± 0.1	2.3 ± 0.1

SUMMARY

Raw kaolinite has been successfully modified with Ag ion and HDTMA. Characterization of the materials validates sustain internal framework of kaolinite even after modification. Furthermore, the HDTMA molecules were proven attached to the kaolinite based on the appearing band on the FTIR spectra of the modified kaolinite. Although Ag ions were unable to be characterized using these instruments, silver modified kaolinite showed a positive bacterial inhibition during DDT assay. Therefore, the appealing capabilities of kaolinite that can incorporate more than one compound enable both HDTMA and Ag ions to be loaded into the kaolinite. Although different concentrations of HDTMA do not contribute to differential inhibition zones, the kaolinite can carry such antibacterial agents that able to synergistically and effectively inhibit bacterial growth of *E. coli* and *S aureus*.

ACKNOWLEDGMENTS

The authors would like to thank Universiti Teknologi Malaysia and the Ministry of Education Malaysia for financial support under Research University Grant (RUG, Vot No: 18H87) and Fundamental Research Grant Scheme (FRGS, Vot No: 4F967).

REFERENCES

1. S.L. Percival, P.G. Bowler, and D. Russell, J. Hosp. Infect. **60**, 1 (2005).
2. L. Ferreira, A.M. Fonseca, G. Botelho, C.A. Aguiar, and I.C. Neves, Microporous Mesoporous Mater. **160**, 126 (2012).
3. K. Kawahara, K. Tsuruda, M. Morishita, and M. Uchida, Dent. Mater. **16**, 452 (2000).
4. D.L. Boschetto, L. Lerin, R. Cansian, S.B.C. Pergher, and M. Di Luccio, Chem. Eng. J. **204**–**205**, 210 (2012).
5. D. Tan, P. Yuan, F. Annabi-Bergaya, D. Liu, and H. He, Sci. Rep. **5**, 1 (2015).
6. C. Ma and R.A. Eggleton, Clays Clay Miner. **47**, 174 (1999).
7. N.A.N.N. Malek, S.A. Ishak, and M.R.A. Kadir, Adv. Mater. Res. **626**, 178 (2013).
8. B. Roshanravan, S.M. Soltani, S.A. Rashid, F. Mahdavi, and M.K. Yusop, Chem. Speciat. Bioavailab. **27**, 44 (2015).
9. R. Slamova, M. Trckova, H. Vondruskova, Z. Zraly, and I. Pavlik, Appl. Clay Sci. **51**, 395 (2011).
10. E. Zarrinabadi, R. Abghari, A. Nazari, and M. Mirjalili, EurAsian J. Biosci. **12**, 1 (2018).
11. J. Deka, L. Satyanarayana, G. V. Karunakar, P.K. Bhattacharyya, and K.K. Bania, Dalt. Trans. **44**, 20949 (2015).
12. W.N. Aryantie, M.Z.A. Awaluddin, and N.A.N.N. Malek, IOP Conf. Ser. Earth Environ. Sci. **276**, 12001 (2019).
13. M. Lai, Z. Liao, Z. Zhou, C. Kao, Y. Li, and H. Wang, Spectrochim. Acta - Part A Mol. Biomol. Spectrosc. **208**, 179 (2019).
14. M. Jeeva, S.K. Lakkaboyana, and W.Z. W.Y., Bull. Geol. Soc. Malaysia **67**, 35 (2019).
15. S. Belkhair, M. Kinninmonth, L. Fisher, B. Gasharova, C.M. Liauw, J. Verran, B. Mihailova, and L. Tosheva, RSC Adv. **5**, 40932 (2015).
16. N.S.S.M. Saad, N.A.N.N. Malek, and C.S. Chong, J. Teknol. **78**, 127 (2016).